Sensors & Transducers, Vol. 249, Issue 2, February 2021, pp. 93-101

Sensors & Transducers
Published by IFSA Publishing, S. L., 2021
http://www.sensorsportal.com

The Novel Computer Aided Diagnostic System on Medical Images for Parameter Calculation

Jong-Ha LEE
Keimyung University, Daegu, South Korea, 40210
Tel.: (82)53-258-3736
E-mail: segeberg@kmu.ac.kr

Received: 12 December 2020 /Accepted: 15 January 2021 /Published: 28 February 2021

Abstract: Recently, the number of Developmental Dysplasia of the Hip (DDH) that occurs during infant and child growth has been increasing a lot. DDH should be detected and treated as early as possible because it hinders infant growth and causes many other side effects. In this study, two modelling techniques were used for multiple training techniques. Based on the results after the first transformation, the training was designed to be possible even with a small amount of data. The vertical flip, rotation, width and height shift functions were used to improve the efficiency of the model. Adam optimization was applied for parameter learning with the learning parameter initially set at $2.0 \times 10e^{-4}$. Training was stopped when the validation loss was at the minimum. No significant difference in angle measurements was found between the model and doctor. The differences in the maximum, minimum, and mean base angles were 6.93, 0 and 1.81 degrees, respectively.

Keywords: non-rigid registration; image-guided surgery, emphysema, laser scanner.

1. Introduction

1.1. Research Background

The incidence of developmental dysplasia of the hip (DDH), which occurs during the developmental period of young children, has been increasing. DDH does not cause external deformities in young children. About 1~2 % of young children on average have DDH, and DDH can be passively detected by medical imaging in 15 % of DDH cases. DDH can be easily treatment if detected within the first year after birth but can incur serious problems if left untreated. Although infants are regularly screened for DDH in the United States, there is not yet a standardized and clear method of DDH screening. South Korea has included DDH in the National Health Screening Program for Infants since 2006. Research has also been started on DDH in South Korea but without clear research standards as is the case in the United States [1-2]. DDH is manually detected by a physician using ultrasonography (US) as a standard practice. However, factors such as the examiner and the system used to perform US can affect the interpretation of the US results. In US-based DDT screening, a medical team measures the acetabulum-femoral head angle on ultrasound scans. A physician then diagnoses DDT based on the angle measurement [3-9]. However, such measurements are subject to errors, which can affect the diagnosis results. US resolution can also have a significant impact on DDT screening results [10-13]. Since DDT is manually detected with the eyes, the resolution and accuracy of ultrasound images can significantly affect screening results [14]. Since DDT is manually screened by a human without a standard guideline, poor resolution can cause large errors. Additionally, a diagnosis is not just made based on an ultrasound image but also on length and angle measurements in different sites [15-19]. Currently, a medical team manually obtains and provides a physician with these measurements. This manual process takes over 10 minutes per image, challenging health professionals in their endeavors to efficiently provide medical services [20-26].

Computational speed has been rapidly increasing due to recent technological advances. The improved performance of graphics processing units (GPU), used in image and video processing, has led to the increasing use of machine learning algorithms used for image processing in industries as well as in the fields of science and medicine. Visual interpretation of medical images is important in the field of medicine. Machine learning algorithms such as convolutional neural networks (CNNs) and improved Resnet 50 are increasingly used in ultrasound image analysis. Related literatures have demonstrated that artificial intelligence (AI)-based image analysis has significantly improved objectivity and productivity in medical settings and that these machine learning algorithms may be used to develop a computer-aided DDH diagnostic system using ultrasound images.

CNNs are a machine learning algorithm used in image analysis and are divided into machine learning and deep learning depending on the level of human intervention. The lower the level of human intervention, the closer an algorithm is to deep learning and the greater the amount of data required. However, it is often the case that there is not enough data to even just train a mode l. If more data are required for deep learning, then human intervention may be increased to resolve the data shortage problem. Thus, we propose a multi-training technique using a user filter.

In this study, we propose a MASK R-CNN-based DDH diagnostic system that can be trained on a small amount of ultrasound image data. The system uses a deep leaning algorithm to automatically calculate the acetabulum-femoral head angle and classify the hip bones of children as normal or abnormal.

1.2. Theoretical Background

1.2.1. Developmental Dysplasia of the Hip

The hip joint consists of an articulation between the acetabulum of the pelvis and the head of the femur. It supports the weight on the pelvis and enables the overall movement of the lower limbs to allow us to stand and run. DDH reduces the contact area between the acetabulum and the femoral head, resulting in increased pressure on the hip joint and thereby promoting degenerative changes of the joint cartilage. Such deformation impedes with smooth joint movements and induces a mismatch between articular surfaces, consequently causing pain or discomfort in daily life and inducing degenerative arthritis by applying an excessive force on the surrounding tissues and causing joint damage. DDH can be effectively treated if detected early in life. It can be easily treated if the treatment is started before an infant is on a walker. An assistive harness, double or triple diapers, Von Rosen splint, or Pavlik harness can be used to treat DDH in infants who are not yet on a walker. An assistive harness is recommended for infants who are less than six-months-old. For infants who are on walkers, a non-surgical method is available in which the hip is properly positioned and fixed in place using plaster bandages. However, infants often do not adapt to the treatment, and surgical procedures such as open reduction in which the fractured bone is put into place through a skin incision and bone correction surgery are more frequently performed.

A natural recovery from DDH without treatment is unlikely for infants. If DDH is not treated during the neonatal period, an infant may have short legs and muscle weakness resulting in limping. A false acetabulum may also form that promotes early degenerative changes. Secondary symptoms may also occur, the most common of which are scoliosis and lumbar pain. Infants with acetabular dysplasia or subluxation may have slightly short lower legs, limp slightly, or show no symptoms at all. However, infants with DDH still require active treatment as they are prone to acetabular cartilage or acetabular labral tears and degenerative changes, and approximately half of them have degenerative arthritis of the hip joint.

1.2.2. AI-based Medical Image Analysis

AI is a branch of computer science that plays a leading role in solving cognitive problems associated with human intelligence such as learning, problem solving, and pattern recognition. AI is currently considered the final stage of computer science. Recent technological advances have improved computational speed and efficiency and led to the emergence of several branches of AI. The advances in network computing have also led to the development of deep learning. There are several branches of AI including machine learning, deep learning, and reinforcement learning, which vary in the level of human intervention.

Machine learning algorithms are used for pattern recognition. Machine learning is a collection of algorithms that are trained on recorded data to make predictions and detect hidden characteristics in variables to concisely represent the data. Unlike previous techniques in which an algorithm designed by a software developer outputs results based on the given input, machine learning produces statistical code through a comparative analysis using a filter to derive an answer based on a previously produced model. It is important to ensure a high quantity and quality of data to increase the accuracy of a machine learning model.

Deep learning is a branch of AI that requires less human intervention compared to machine learning and is a more advanced form of machine learning. Whereas machine learning detects characteristics in answers during the training phase and infers results for other examples, deep learning analyzes a large amount of data without human intervention and infers results on its own. Instead of forming related sets as is done by machine learning algorithms, deep learning uses nonlinear algorithms to produce a model that detects associations between inputs. Deep learning can make predictions about data whose complexity is beyond human cognitive ability or the analytical ability of existing software-based techniques or machine learning algorithms to be analyzed. Since deep learning requires more data than machine learning, it is appropriate for use in fields where a large amount of data are available.

1.3. Previous Research

1.3.1. Standardized Method of Measurement for DDH

Two methods are available to detect DDH: physical examination and US. In a physical examination, DDH may be diagnosed based on unequal skin folds in the femoral region between the left and right thighs. The Galeazzi test may also be used to diagnose DDH, which checks for a discrepancy in the height of the knees when an infant is lying on a flat surface with their knees up. In the Ortolani test, a click sound that can be heard when the dislocated femoral head is placed back in the pelvis is checked. An infant is first laid on the floor, and the knee and hip joints are bent. The femoral head is then pushed upward while the thighs are spread apart to hear a clicking sound and feel the femoral head fitting into the acetabulum. In the Barlow's test, dislocation is induced by pushing the femoral head while the thighs are bringing the thighs together with the hip joint adducted. These are the physical screening methods for DDH.

There are two methods of radiological examination of DDH: X-rays and US. Before an X-ray examination, it is necessary to check that the femoral head is in contact with the pelvic bone. Since the femoral head consists of cartilage in the neonatal period, it cannot be observed on X-rays. Although the femoral head is observed on X-rays starting 6-7 months after birth, US is more appropriate for early diagnosis. In US, which is the main topic of this study, ultrasound scans of the hip joint where the triradiate cartilage can be observed are obtained in the coronal plane while the ilium is placed horizontally. The ilium must be five degrees below the horizontal axis. A and β angles are measured to make a diagnosis.

1.3.2. Edge Detection Filter

There are many unnecessary areas on ultrasound scans. Unlike CT scans, ultrasound scans lack clear feature points and contain many areas that look similar and hinder feature detection. Unnecessary parts must be removed to extract feature points. In this study, edge detection was used as a filtering method. Since ultrasound scans are grey-scale images, edge detection can be performed without processing the ultrasound scans. Edge detection is the process of detecting edges on images. Edges are a sequence of points on an image where the intensity of a pixel drastically changes from the threshold value. Such changes in pixel intensity can be detected using derivatives. The first-order derivative captures the magnitude of the slope, and the second-order derivative captures the sign of the slope. Masks are used in edge detection, which are filters that have the same effect as a differential operator. The Sobel, Prewitt, and Roberts operators can be used in edge detection using first-order derivatives. The Sobel and Prewitt operators are less sensitive to noise and have a slow computational speed. The Roberts operator has a fast computational speed and can detect edges with high accuracy but is sensitive to noise. Edge detection using first-order derivatives can detect horizontal and vertical edges. Second order derive masks include the Laplacian mask and Canny mask. The Laplacian mask reduces noises by Gaussian smoothing and then performs the Laplacian of Gaussian operation. The Canny mask reduces noise by smoothing using a Gaussian filter, detects edges by performing a mask operation, and then applies non-maximum suppression to remove non-edges.

1.4. Objective

Fig. 1 shows diagram of the proposed system. As explained in previous studies, DDH must be diagnosed early in infants, and the most effective method of DDH detection is US. However, a relatively small amount of data can be obtained from ultrasound scans of infants compared to the amount of time and effort put into the data acquirement due to the low age of infants and the nature of the ultrasound scans. Even then, only a small portion of the obtained data are of acceptable quality. Ultrasound scans must be clear enough for examination with the naked eyes and the angle between the ilium of the hip joint and the baseline must measure 5 degrees or less to be used in an analysis. Currently, a medical team manually examines each image to determine its acceptability. The team measures and records lengths and angles on ultrasound scans using a computer to determine whether an infant has DDH. This is a highly time-consuming process. Owing to the active research on AI, AI may detect DDH in ultrasound scans more effectively than do existing programs. Ultrasound scans have many similar areas; therefore, it is difficult to detect features from ultrasound scans based on a naked-eye examination alone. CNNs can extract features from ultrasound scans. A large amount of data are required to perform machine learning or deep learning. Thus, it is difficult to effectively use AI algorithms without sufficient data. In most cases, data are lacking or not processed. A method to train a machine learning or deep learning model with a small amount of data and obtain a large amount of processed data is needed. We proposed a MASK-R-CNN-based ultrasound DDH detection method that requires increased human intervention and reduced data requirements. The method produces a seed model that can process a large amount of data from a small initial dataset at a research laboratory or corporate hospital to develop an initial AI environment.

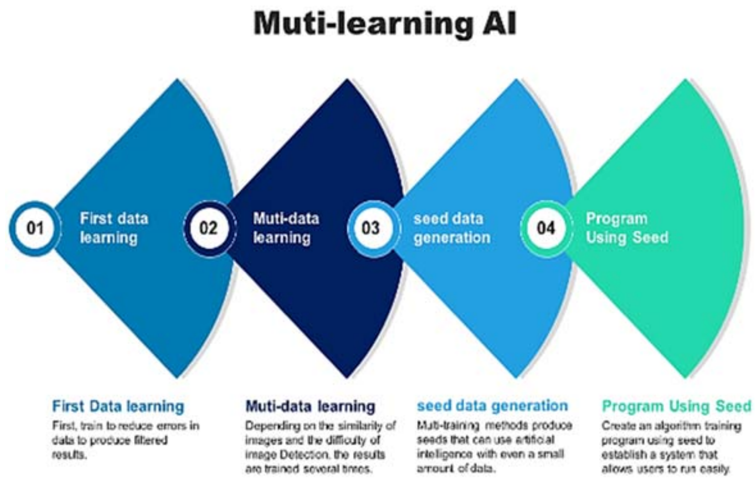

Fig. 1. The goal of the system.

2. Materials and Methods

2.1. Method

This study is aimed at developing a system that uses a multi-training method to process unprocessed data to increase the user accessibility. Previously, DDH was diagnosed by detecting the areas containing the ilium and acetabular roof, measuring the angles of the ilium and acetabular roof, and using a machine learning algorithm to make a prediction based on these angle measurements. Instead of measuring the angles from the ilium and acetabular roof following area detection, the areas containing the α and β angles of the ilium and acetabular roof are detected to measure the angles.

The Mask R-CNN method is used to first segment the shapes on ultrasound images formed by the ilium and acetabular head. Two points on the ilium and three points for calculating the α and β angles (four points in total with one overlapping point) are used to determine the acceptability of an image. The points are connected to obtain meaningful values for DDH diagnosis.

Based on a previous study in which segmentation and key points were used to extract a large amount of information from a given amount of data and achieved higher machine learning performance, the four points on the ilium and acetabular roof and segmentation were used to produce a deep learning model.

2.1.1. Segmentation Environment

Mask R-CNN was used for segmentation. Mask R-CNN is an extension of Fast R-CNN with the addition of a Mask-head. The Mask head is first used to detect the areas corresponding to the ilium and acetabular roof. A ResNet algorithm consisting of 50 layers modified using the background algorithm of Mask R-CNN. The ROIAlign and Feature Pyramid Network (FPN) were used for feature extraction.

2.1.2. File Conversion

The US data obtained from the participants were in the DICOM format. The DICOM files included information about ultrasound scans (date, type of equipment, imaged area, and patient) and image data. For personal information protection and memory efficiency reasons, this information was removed, and the ultrasound images were converted to 256-bit greyscale images.

2.1.3. Layer Extraction

A model was trained on ultrasound scans for segmentation. An area to be masked for the first training phase must be marked. The area is marked using the CVAT program developed by the MIT.

2.1.4. First Training

Polypoints were assigned to the areas on an image that contain the ilium and acetabular roof using the point selection tool. Points were assigned across a sequence of images. An extraction tool can be used to obtain XML or JSON files containing point records. The obtained XML and image files were used to train the first model.

2.1.5. Second Training

A model was trained using the output from the previously trained model. Using CVAT, the start and end of the ilium and the top and bottom of the acetabular roof were marked with dots. The start of the ilium was estimated based on a naked-eye examination, and the end of the ilium was designated to a point near the intersection between the three lines. The top of the acetabular roof was designated above the line extending to the acetabular roof. The bottom of the acetabular roof was designated below the line extending to the acetabular roof. Refer to the figure below for these points.

2.1.6. Final Results

Once the second training was complete, the first and second models were used to predict the angles and lengths of the ilium and acetabular roof. Hence, an AI system was developed that could assist physicians in diagnosing DDH based on these predicted values.

3. Results

A total of 2,692 ultrasound scans collected from 2016 and 2019 at Dongsan Medical Center were obtained. Of these, 1,242 were acceptable for use in the analysis. 321 of these scans were randomly selected and then arbitrarily divided into a training dataset containing 288 scans and a test dataset containing 33 scans.

To produce a machine learning model, the multi-training algorithm proposed in this study. The training parameter was set to $2.0e^{-3}$, and the model was trained until the validation loss was at the minimum. The trained model was then tested using 920 scans.

The 322 ultrasound scans obtained from Dongsan Medical Center were arbitrarily divided into a training dataset containing 288 scans and a validation set containing 33 scans. Of the total 920 scans, 389 were deemed acceptable (could be clearly interpreted by an orthopedic doctor at Dongsan Medical Center). The system correctly detected DDH in 369 out of the 389 scans, achieving a detection accuracy of 94.86 %.

3.1. Acceptable Data

Less than 20 % of all unprocessed data collected by a medical team is deemed acceptable due to the movements of the patient and the US equipment. Collecting acceptable data from infants is even more difficult. In this study, 1,242 of 2,692 raw scans were selected for use in the experiment (First screening). Next, from the test dataset containing 920 scans, 389 scans deemed acceptable for interpretation were selected to measure the performance of the system (Second screening).

Acceptable scan (Left) Unacceptable scan in the second screening (Middle) Unacceptable scan in the first screening (Right).

3.2. Method of US Scan Acquirement

Ultrasound scans were obtained from infants aged less than two years using HD7-XE from Philips. At least 30 scans were obtained per infant.

3.3. Performance Classification

To measure the performance of the system, the model's output was classified as appropriate detection, fail detection, different result, false image, inappropriate detection, or insufficient image. 'OK' indicated that the system produced normal outputs for normal data. 'Error' indicated that although an output was produced, an image was deemed inappropriate since the base angle value was not within the normal range. 'N/A' indicated that an output could not be produced due to non-available values.

The detection results of the total 920 scans were as follows: 'Appropriate detection' for 413 scans, 'Fail detection' for 98 scans, 'Different result' for 30 scans, 'False image' for 336 scans, 'Inappropriate detection' for 9 scans, and 'Insufficient image' for 34 scans. The figure below shows a bar graph the detection results starting with 'Appropriate Detection' from the far left followed by 'False Image', 'Different Result', 'Insufficient Image', 'Fail Detection', and 'Inappropriate Detection'. Fig. 2 shows the detection results.

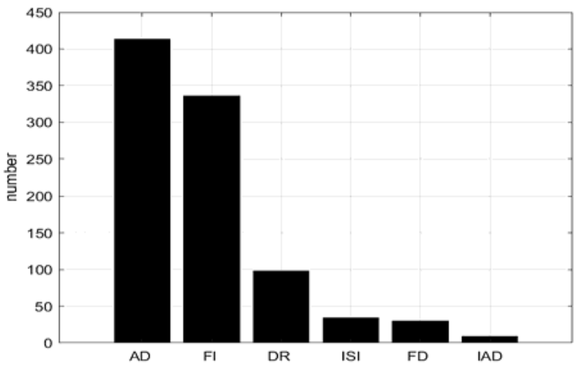

Fig. 2. Detection results.

3.4. Measuring System Performance

Performance parameters were used to assess the systems' performance. Since the answer must be divided into true or false, the classifier was also divided into OK (True) and error. A 2×2 matrix could then be created (Table 1). Of the total 510 scans excluding the ones classified as 'N/A', 320 were true positives (TPs), 48 were false positives (FPs), 49 were false negatives (FNs), and 93 were true negatives (TNs).

Table 1. 2×2 matrix based on true/false classification.

	AI OK	AI Error
Doctor OK	320 scans (TP)	48 scans (FP)
Doctor Error	49 scans (FN)	93 scans (TN)

3.5. System Performance Parameters

Based on the above classification, performance parameters could be calculated (Table 2). The equations below were used to calculate precision, recall, accuracy, F1 score, and fall-out. Precision was calculated at 0.87, recall at 0.87, accuracy at 0.81, F1 score at 0.87, and fall-out at 0.34.

Table 2. The values of the performance parameters (%).

	Value
Precision	$8.796e^{-3}$
Recall	$8.672e^{-3}$
Accuracy	$8.098e^{-3}$
F1 score	$8.684e^{-3}$
Fall-out	$8.404e^{-3}$

The vertical flip, rotation, width and height shift functions were used to improve the efficiency of the model. Adam optimization was applied for parameter learning with the learning parameter initially set at $2.0 \times 10e^{-4}$. Training was stopped when the validation loss was at the minimum. Fig. 3 shows the results.

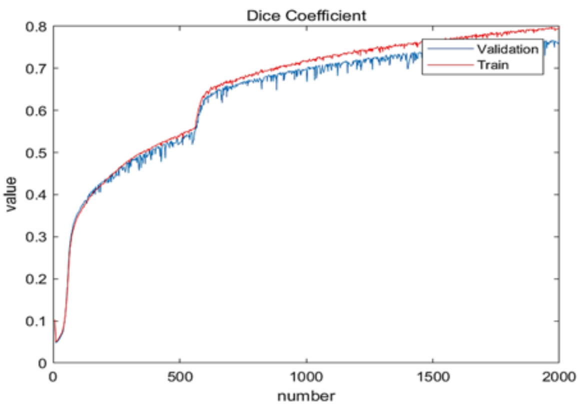

Fig. 3. Dice coefficients for the validation and training datasets.

Dice coefficients share a similar concept as intersection over union (IOU). They are calculated by dividing the area of overlap by the total number of pixels. They are commonly used to assess the accuracy of edge prediction and essentially represent the accuracy of a predicted bounding box. Dice coefficients close to 1 indicate good performance whereas those close to 0 indicate poor performance. Fig. 4 shows the results.

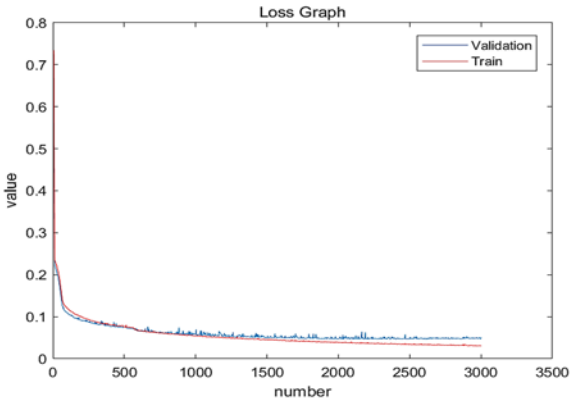

Fig. 4. Loss values for the validation and training dataset

The loss value graph shows loss values. Loss values are closer to 0 when a model makes correct predictions.

3.6. Measurement Comparison

No significant difference in angle measurements was found between the model and doctor. The differences in the maximum, minimum, and mean base angles were 6.93, 0, and 1.81 degrees, respectively (Fig. 5).

The differences in the maximum, minimum, and mean α angle were 19.78, 0.01, and 3.56 degrees, respectively (Fig. 6).

The differences in the maximum, minimum, and mean β angle were 25.92, 0.01, and 4.51 degrees, respectively (Fig. 7).

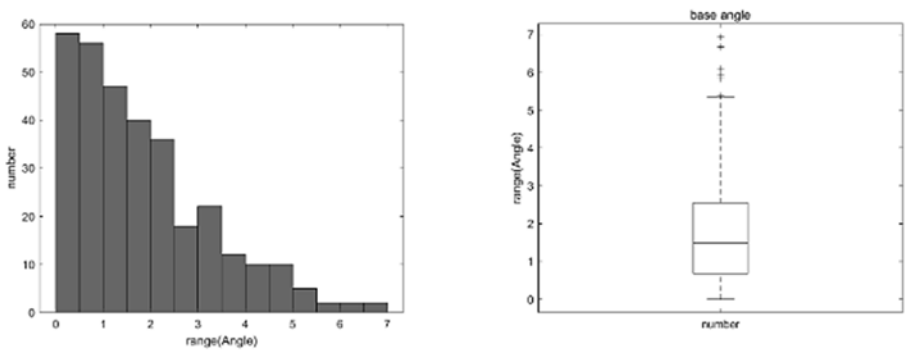

Fig. 5. Base angle range.

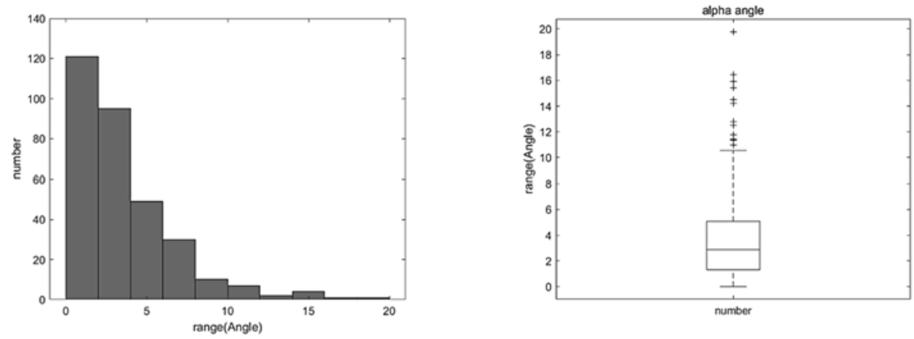

Fig. 6. α angle range.

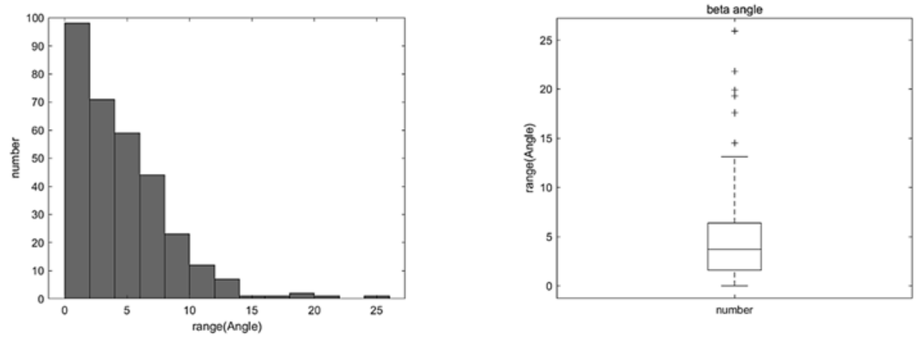

Fig. 7. β angle range.

4. Discussion

In this paper, the training was conducted with a smaller amount of data than the existing training method, and it was confirmed that the performance was better than the existing method when the multi-training technique presented in this paper was used with ultrasonic photography that is more complex than other image images. This technique is expected to be used in small laboratories or development teams that need to build AI with a small amount of data and can be used as a seed that training on a large of data based on this technique.

The techniques used in the paper are divided into machine learning and deep learning depending on the degree of user intervention in artificial intelligence. In the original image, train the part used for judgment first. It removes all areas other than the detected areas to enhance the filtering of noise. Re-training the part of the angle corresponding to the angle. Re-training the points corresponding to the angle. It is designed to detect parts that are needed even with less data than conventional training methods.

2,692 sheets of data were used in the experiment, but due to the nature of the ultrasound, all data that were highly swayed, noisy, or could not be verified by the human eye were excluded. As a result, the total number of data used for training was 1,242. Of these, 321 were brought in as data for modeling and construction. The data to be tested through the generated modelling was classified into 920 chapters. First of all, training data for modeling formation and test data for learning stabilization are required for modeling construction. We trained with 288 training data and 33 test data respectively. The second training was trained with the converted file of the data used for the first training. The most difficult thing about collecting effective data was that the subject was infants and that ultrasound had bigger artefacts than other medical images such as CT and MRI. Although medical staff with more than five years of experience filmed, the normal data acquisition rate was less than 50 percent. Because of the addition of medical elements, the photos were classified into six categories by medical measurement methods. The six categories factors actually require complex criteria. For quantitative measurement, the answer sheet for each image of doctors and AI was fixed with OK, Error, and NA. OK stands for normal range values for normal data. Error is normal data, but the base angle is not the normal range, which means an abnormal image. NA means when a value cannot be derived as non-available. Performance measurement methods were distinguished by general model evaluation classification indicators. 510 data were detected except for NA options that doctors could not detect. OK and Error of choice of doctor and artificial intelligence were calculated as a total of four based on two correct answers. Performance evaluation of AI used a performance evaluation index, Dice coefficient, and loss graphic, and the result was very good. The medical performance compared the differences in alpha beta angles. Comparing to the average, there was a difference of less than 4 degrees. This is a good result because it is the range of differences that occur on average when measuring the same picture between doctors.

Conclusions

Recently, the number of hip dysplasia (DDH) that occurs during infant and child growth has been increasing. DDH should be detected and treated as early as possible because it hinders infant growth and causes many other side effects. DDH's standard screening method is to utilize Ultrasonography (US). However, the Ultrasonography (US) may differ in the reading results depending on the proficiency of the physician. It also takes a lot of skill to define DDH levels depending on the quality of the Ultrasonography (US). In order to improve the doctor's proficiency, many patient cases should be encountered and large-capacity Ultrasonography (US) should be obtained. However, due to the nature of infants and toddlers, only 2 to 10 percent of the photos taken can be used as meaningful photos. Currently, significant photographs are used by doctors to determine DDH in ultrasonic images, such as the angle of the Acetabulum-Femoral head for ultrasonic image reading. However, this method causes a lot of errors because the doctor works manually. Recently, machine learning techniques using Convolutional Neural Networks (CNN) and improved Resnet50 have been widely used for ultrasound image analysis. Research shows that computer-aided image analysis greatly improves objectivity and productivity at medical sites. This shows that the DDH computer-aided diagnostic algorithm through ultrasound images can solve difficult challenges in orthopedics.

In this paper, we proposed a computer-aided diagnostic algorithm that can automatically measure and diagnose DDH using CNN. In this study, the algorithm was designed to automatically calculate the angle of the acetyaboulum-femoral head for normal/nonnormal reading of the infant hip joint and to perform diagnosis automatically by deep learning of existing images. Experiments have shown that the speed and accuracy of diagnosis are improved compared to doctors.

Acknowledgements

This research is supported by "The Foundation Assist Project of Future Advanced User Convenience Service" through the Ministry of Trade, Industry and Energy (MOTIE) (R0004840, 2018) and Basic Science Research Program through the National Research Foundation of Korea(NRF) funded by the Ministry of Education (NRF-2017R1D1A1B04031182) the Ministry of Trade, Industry and Energy(MOTIE) and Korea Health Technology R&D Project through the Korea Health Industry Development Institute (KHIDI), funded by the Ministry of Health & Welfare, Republic of Korea (grant number : HI17C2594).

References

[1]. Webster J. G., Encyclopedia of Medical Devices and Instrumentation, *John Wiley & Sons,* New York, 1988.

[2]. Geddes L. A., Baker L. E., Principles of Applied Biomedical Instrumentation, *John Wiley & Sons,* New York, 1989.

[3]. Cameron J. R., Skofronick J. G., Physics of the Body, *Medical Physics Publishing Corporation*, 1999.

[4]. Perloff D., Grim C., Flack J., Frohlich E. D., Hill M., M. McDonald, *et al*., Human blood pressure determination by sphygmomanometry, *Journal of Amreican Heart Association*, Vol. 88, Issue 5, 1993, pp. 2460-2470.

[5]. O'Grady N. P., Alexander M., Dellinger E. P., Gerberding G. L., Heard S. O., Maki D. G., *et al*., Guidelines for the prevention of intravascular catheter-related infection, *Clinical Infectious Diseases*, Vol. 52, Issue 9, 2011, pp. e162-e193.

[6]. Drzewiecki G. M., Melbin J., Noordergraaf A., The Korotkoff sound, *Ann. Biomedical Eng.*, Vol. 17, 1989, pp. 325-359.

[7]. Moraes J. C. T. B., Cerulli M., Ng P. S., Development of a New Oscillometric Blood Pressure measurement System, in *Proceedings of the IEEE Computers in Cardiology Conf.*, Vol. 26, 1999, pp. 467-470.

[8]. Wax D. B., Lin H. M., Leibowitz A. B., Incasive and concomitant noninvasive intraoperative blood pressure monitoring, *Anesthesiology*, Vol. 115, 2011, pp. 973-978.

[9]. Verkruysse W., Svaasand L. O., Nelson J. S., Remote plethysmographic imaging using ambient light, *Optics Express*, Vol. 16, Issue 26, 2008, pp. 21434-21445.

[10]. Poh M. Z., McDuff D. J., Picard R. W., Non-contact, automated cardiac pulse measurements using video imaging and blind source separation, Optics Express, Vol. 18, Issue 10, 2010, pp. 10762-10774.

[11]. Poh M. Z., McDuff D. J., Picard R. W., Advancements in noncontact, multiparameter physiological measurements using a webcam, *IEEE Transactions on Biomedical Engineering,* Vol. 58, Issue 1, 2011, pp. 7–11.

[12]. McDuff D., Gontarek S., Picard R. W., Improvements in remote cardiopulmonary measurement using a five band digital camera, *IEEE Transactions on Biomedical Engineering*, Vol. 61, Issue 10, 2014, pp. 2593–601.

[13]. Gesche H., Grosskurth D., Küchler G., Patzak A., Continuous blood pressure measurement by using the pulse transit time comparison to a cuff-based method, *European Journal of Applied Physiology*, Vol. 112, Issue 1, 2012, pp. 309-315.

[14]. Turk M., Pentland A., Eigenfaces for recognition, *Journal of Cognitive Neuroscience*, Vol. 3, Issue 1, 1991, pp. 71–86.

[15]. Zhao W., Chellappa R., Phillips P. J., Rosenfeld A., Face recognition: A literature survey, *ACM Computing Surveys,* Vol. 35, Issue 4, 2003, pp. 399–458.

[16]. Kamarainen J. K., Kyrki V., Kälviäinen H., Invariance Properties of Gabor filter-based features-overview and applications, *IEEE Transactions on Image Processing*, Vol. 15, Issue 5, 2006, pp. 1088–1099.

[17]. Wiskott L., Fellous J. M., Kuiger N., Malsburg C., Face Recognition by Elastic Bunch Graph Matching, *IEEE Transactions on Pattern Analysis and Machine Intelligence*, Vol. 19, Issue 7, 1997, pp. 775–779.

[18]. Brown L. G., A Survey of Image Registration Techniques, *ACM Computing Surveys*, Vol. 24, Issue 4, 1992, pp. 325-376.

[19]. Zitova B., Flusser J., Image Registration Methods: A Survey, *Image and Vision Computing*, Vol. 21, Issue 11, 2003, pp. 977-1000.

[20]. Rangarajan A., Chui H., Bookstein F., The Softassign Procrustes Matching Algorithm, *Medical Image Analysis*, Vol. 4, 1999, pp. 1-17.

[21]. Besl P. J., Mckay N. D., A Method for Registration of 3-D Shapes, *IEEE Transaction Pattern Analysis and Machine Intelligence*, Vol. 14, Issue 2, 1992, pp. 239-56.

[22]. Chui H., Rangarajan A., A New Point Matching Algorithm for Non-Rigid Registration, *Computer Vision and Image Understanding*, Vol. 89, Issue 2-3, 2003, pp. 114-141.

[23]. Rangarajan A., Gold S., Mjolsness E., A Novel Optimizing Network Architecture with Applications, *Neural Computing*, Vol. 8, Issue 5, 1996, pp. 1041-1060.

[24]. Myronenko A., Song X., Carreira-Perpinan M. A., Non-rigid Point Registration: Coherent Point Drift, *Advances in Neural Information Processing Systems*, Vol. 19, 2007, 1009-1016.

[25]. Belongie S., Malik J., Puzicha J., Shape Matching and Object Recognition Using Shape Contexts, *IEEE Transaction Pattern Analysis and Machine Intelligence*, Vol. 24, Issue 4, 2002, pp. 509-522.

[26]. Zheng Y., Doermann D., Robust Point Matching for Nonrigid Shapes by Preserving Local Neighborhood Structures, *IEEE Transaction Pattern Analysis and Machine Intelligence*, Vol. 28, Issue 4, 2006, pp. 643-649.